Low frequency modifications of seismic background noise due to interaction with oscillating fluids in porous rocks

M. FREHNER, S. SCHMALHOLZ
Geological Institute, ETH Zurich, Switzerland, frehner @ erdw.ethz.ch, +41 44 632 88 72

Y. PODLADCHIKOV
Physics of Geological Processes, University of Oslo, Norway

R. HOLZNER
Spectraseis AG, Giessereistrasse 5, CH-8005 Zurich, Switzerland

Abstract

Studies of passive seismic data in the frequency range below 20Hz have shown that the frequency content of the ever-present seismic background noise changes above hydrocarbon reservoirs. Different explanations for this observation have been proposed. In this study, it is shown that oscillating pore fluids, i.e. oil, can change the frequency content of the seismic background noise. A 1D wave equation is coupled with a linear oscillator equation, which represents these pore fluid oscillations. The resulting linear system of equations is solved numerically with explicit finite differences and different types of external sources and boundary conditions are applied. It is shown that the elastic wave initiates oscillations of the fluid drops. The oscillatory energy of the pore fluid is transferred continuously to the elastic rock matrix. In consequence, seismic waves in the elastic rock contain the eigenfrequency of the pore fluid oscillations in addition to the frequency content of the background noise. The presented model is considered as a possible explanation for observed spectral modifications above hydrocarbon reservoirs.

Key points of this study

- Change of frequency content of seismic background noise above hydrocarbon reservoirs observed around the world
- Physical explanation subject to current discussions
- Numerical model developed to simulate oscillations of trapped oil blobs in pores coupled with elastic wave propagation.
- Incident elastic wave initiates oscillations of pore fluid.
- Micro-scale pore fluid oscillations can change frequency content of seismic background noise.

Data Examples

Spectraseis survey for Petrobras, Potiguar Basin, Brazil, 2004: Spectra of continuous passive measurements of seismic background noise above (red) and nearby (blue) a proven oil reservoir. The measurement above the reservoir shows additional energy in the low frequency range.

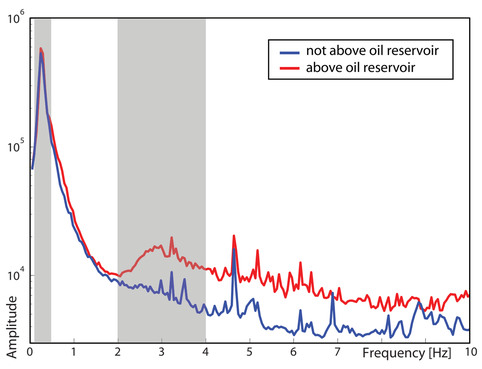

Spectraseis survey for RAG, Voitsdorf area, Austria, 2005: Measurements of seismic background noise are done with a three-component-seismometer. Shown are spectra of the vertical component of two different measurement locations, one above a known oil reservoir (red) and one away from the reservoir (blue).

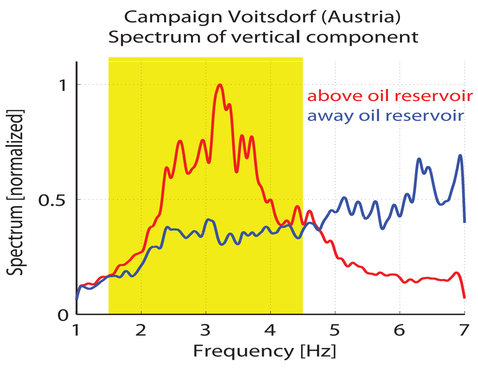

Spectraseis survey for RAG, Voitsdorf area, Austria, 2005: Measurements of seismic background noise are done with a three-component-seismometer. Ratio between vertical and the two horizontal spectra shows additional energy in the low frequency range (upper figure) above the oil reservoir that is known from an active seismic survey (lower figure).

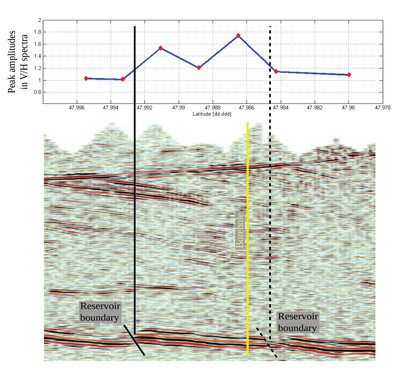

Taken from Dangel et al., 2003: Spectra of continuous passive measurements of seismic background noise above (red) and nearby (blue) proven oil reservoirs. All measurement above reservoirs shows additional energy in the low frequency range compared to measurements nearby. a) Jordan, b) Italy, c) Ukraine and d) Morocco

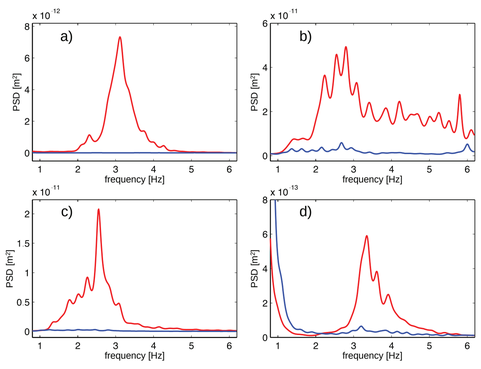

Spectraseis survey for Pemex, Burgos Basin, Mexico, 2006: Spectra of continuous passive measurements of seismic background noise above (red) and nearby (blue) a proven oil reservoir Linear representation of the spectra and logarithmic representation in the inlay. The measurement above the reservoir shows additional energy in the low frequency range..

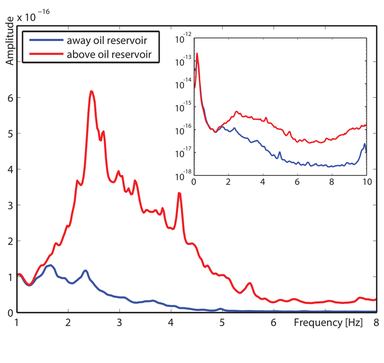

Application

Spectral modifications of seismic background noise in the frequency range below 20Hz have been observed above hydrocarbon reservoirs in many places around the world (e.g. Dangel et al.). These spectral modifications are used as direct hydrocarbon indicator (Holzner et al., 2005; Akrawi and Bloch, 2006; Suntsov et al., 2006). A general workflow (e.g. Spectraseis AG) starts with data acquisition and ends with two dimensional maps indicating hydrocarbon potential.

- Long-time continuous passive seismic measurements
- Data processing in time domain
- Fourier transformation
- Data processing in Fourier domain
- Spectral Analysis of data
- Data interpretation, production of maps

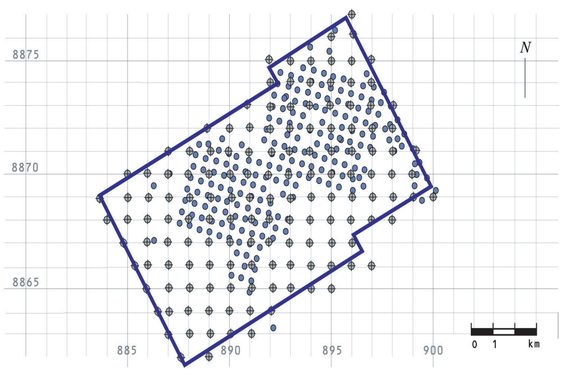

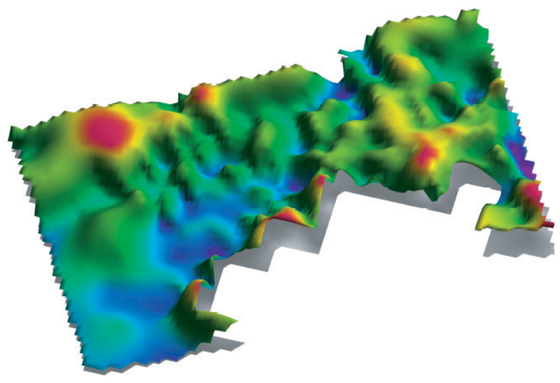

Working hypotheses

The physical explanation for the observed spectral modifications is the subject of current discussions (Graf et al. 2007). Seismic attenuation phenomena in poro-elastic media, subsurface reflection patterns, resonant amplification due to oscillations and phase transition effects (Suntsov et al. 2006) have been discussed as possible causes. The ongoing research project can be divided into two main branches.

Resonant amplification
Certain frequencies of incoming waves are amplified due to an oscillation process at the pore scale. Frequencies around the resonance frequency show higher amplitudes in the velocity spectra.

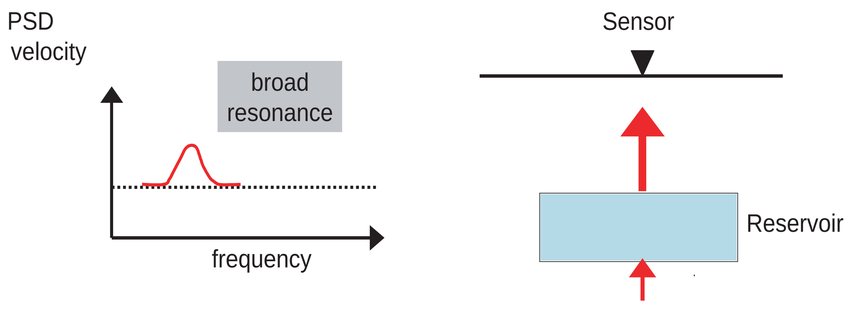

Resonant scattering
Incoming waves are reflected at the surface and the reservoir due to heterogeneities.
The characteristic two-way travel time between reservoir and surface causes peaks in the velocity spectra.

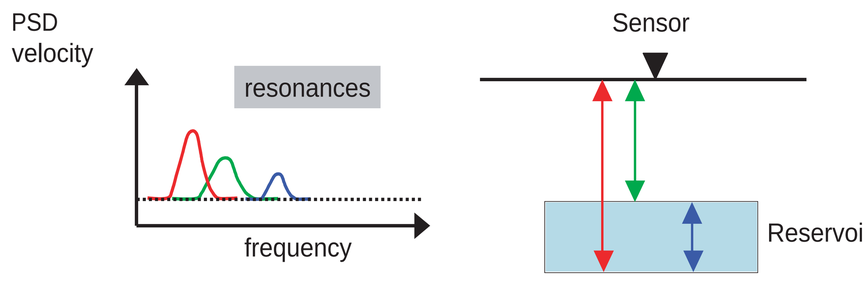

Eidgenössische Technische Hochschule Zürich
Swiss Federal Institute of Technology Zurich
PHYSICS OF GEOLOGICAL PROCESSES
Spectraseis

Pore fluid oscillations

To understand first order effects, pore shapes are simplified (Holzner, 2007, Hilpert, 2007). Yellow fluid fills the pore only partially. That allows oscillations of the fluid. Surface tension acts as the restoring force driving the oscillations. Geometries on the left and the right result in a nonlinear relation between displacement and restoring force, i.e. a nonlinear oscillation. Geometry in the middle results in a linear oscillation.

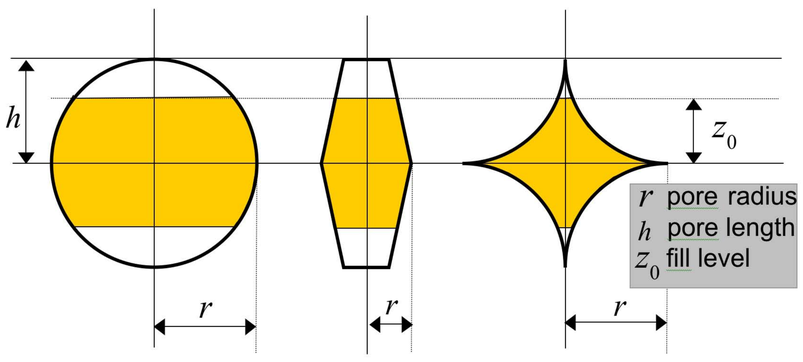

In this study, only the linear geometry is considered. Given are the surface tension force, spring constant, mass and eigenfrequency.

$$F = 2\pi\gamma r\left(\frac{z}{h}-1\right)\ ,\ f = \frac{\partial F}{\partial z} = 2\pi\gamma\frac{r}{h}$$

$$m \approx \frac{2}{3}\pi r^2 h\rho^f\ ,\ \omega_0 = \sqrt{\frac{f}{m}} = \sqrt{\frac{6\gamma}{h^2 r\rho^f}}$$

Coupling of pore fluid oscillations with elastic rock

Oscillatory behavior of pore fluid is coupled to standard elastic wave propagation equations. This is done using Hamilton's variational principle applied to the Langrangian functional (Bourbie et al., 1987). Two partial differential equations result. The schematic rheological model for the coupling between elastic deformation and pore fluid oscillations consists of an elastic bar with Young's modulus E and a linear oscillator of eigenfrequency ω_0. Two displacements have to be considered, one for the elastic subsystem u^s and one for the oscillatory fluid subsystem u^f.

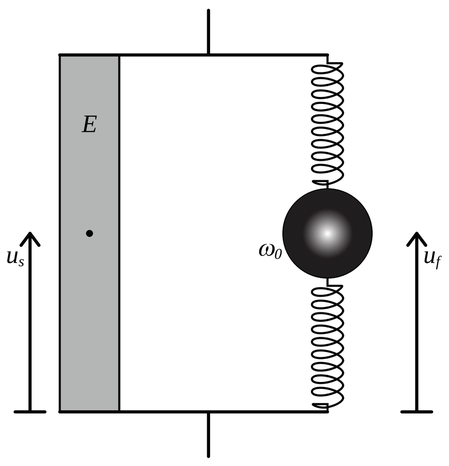

Coupled linear system of equations for two unknown displacements u^s and u^f.

$$S\phi\rho^f\frac{\partial^2 u^f}{\partial t^2} = -S\phi\rho^f\omega_0^2\left(u^f - u^s\right)$$

$$(1-\phi)\rho^s\frac{\partial^2 u^s}{\partial t^2} = \frac{\partial}{\partial x}\left(E\frac{\partial u^s}{\partial x}\right) + S\phi\rho^f\ddot{\alpha}$$

Numerical model setup

Model equations are discretized using finite difference method on a staggered grid and an explicit predictor-corrector method in time (Virieux, 1986). One-dimensional model setup for numerical simulations consists of three receivers R1-R3 and one source S identical with position of receiver R1. The model is homogeneous and is described by coupled system of Equations. Lower and upper boundaries can be rigid (zero displacement) or non-reflecting (Ionescu and Igel, 2003). All physical parameters used are listed in the table.

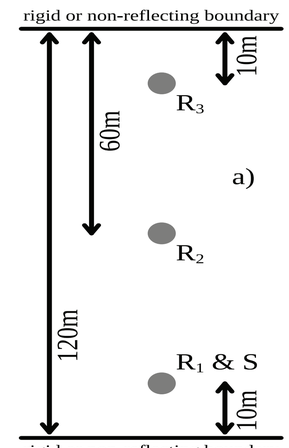

Symbol	Value
h	$5 \cdot 10^{-3}$ m
r	10^{-3} m
γ	10^{-3} N m^{-1}
ω_0	18.85 (= 3Hz · 2π)
ρ^f	800 kg m^{-3}
ρ^s	2800 kg m^{-3}
E	$2 \cdot 10^{10}$Pa
ϕ	0.3
S	0.9

Results

Energy conservation and transfer

In the presented model four different energies exist. Their evolution is plotted for a time interval of two seconds. In this simulation both boundaries were rigid. No external source was applied but a Gaussian curve for the solid velocity was used as initial condition. Total energy, i.e. the sum of all energies (thick black line) stays constant over time. Energy in the system is conserved. Internally energy is transferred between solid and fluid.

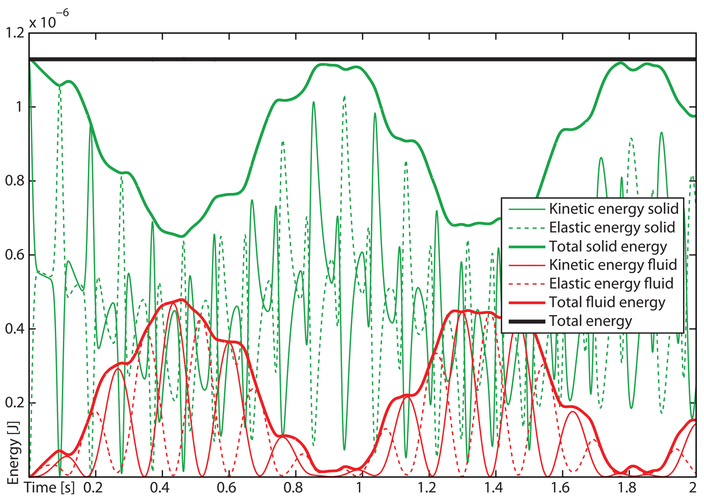

Incident elastic wave

In this simulation both boundaries were non-reflecting. External source applied at position S is a Gaussian curve in time with a very short width that is symmetric at 10 seconds. The spectrum of this source function is shown in the inlay. At R_3 both fluid and solid velocities are recorded and spectrograms are calculated. Due to the algorithm calculating the spectrogram, the signal of the external source is visible for 10 seconds (between 5 and 15 seconds). Over this interval the spectrogram of the solid velocity (upper figure) shows a trough at the eigenfrequency of the fluid oscillations. The second half of the spectrogram shows a peak at this frequency. The spectrogram of the velocity of the fluid (lower figure) always shows a peak at the eigenfrequency of the fluid oscillations.

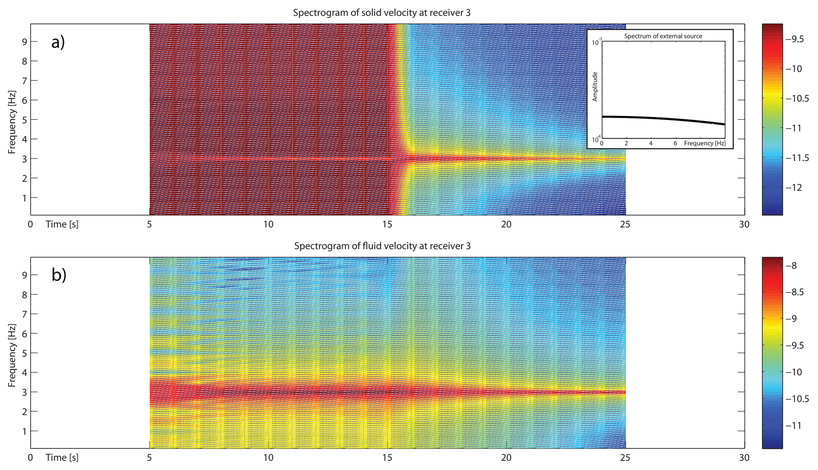

Resonace curves

In these simulations both boundaries were non-reflecting. The external sources applied at S are sinusoidal curves with changing frequencies. At R_3 both fluid and solid velocities are recorded and spectra are calculated. In both spectra two distinct peaks are present, one at the external frequency, and one at the eigenfrequency of the fluid oscillations. These two spectral peaks are picked for each simulation. That leads to the four resonance curves shown. The closer the external frequency is to the eigenfrequency of the pore fluid oscillations the stronger the response of the fluid phase becomes, both at the eigenfrequency (b) and at the external frequency (d). The response of the solid phase at the eigenfrequency of the pore fluid oscillations (a) is almost proportional to the response of the fluid phase at the same frequency. The resonance curve for the solid response at the external frequency (c) is characterized by a trough at the eigenfrequency of the pore fluid oscillations.

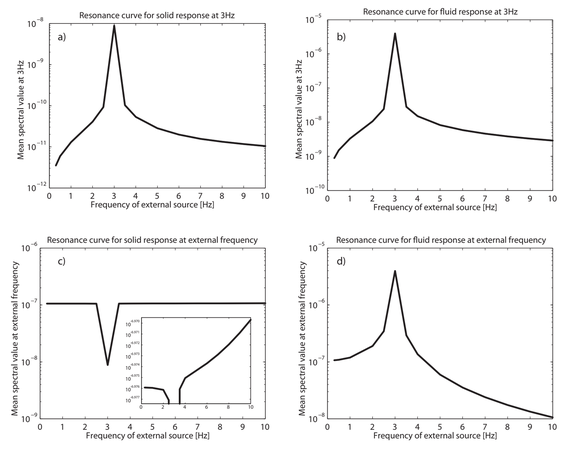

Numerical spectra over time

Spectra of solid velocity at receiver R_3 are shown for a 50m thick porous layer. Different spectra are calculated after different simulation lengths. Longest time signal is 120s (black spectra), shortest is 3.5s (red spectra). Dash-dotted vertical line: Frequency of external force; Solid vertical line: Eigenfrequency of pore fluid oscillations.

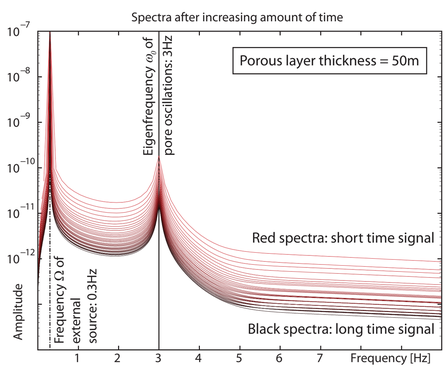

Changing thickness of reservoir

Time evolution of amplitude ratio between 3Hz-peak and 0.3Hz-peak in the spectra are represented double-logarithmically. Different colors represent different porous layer thicknesses. Spectra are calculated with the solid velocity time signal at receiver R_3.

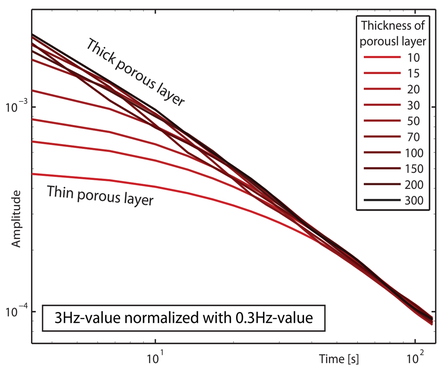

Discussion / Conclusions

At the moment of incidence of the elastic wave, the fluid immediately starts to oscillate with its eigenfrequency. To initiate the oscillations, energy at the eigenfrequency of the oscillations is transferred from the solid to the fluid. Therefore a trough in the spectrogram of the solid velocity occurs at this frequency. After the elastic wave has passed, the fluid continues to oscillate with its eigenfrequency. Energy at the eigenfrequency of the oscillations is continuously transferred from the fluid to the solid.

The trough in the resonance curve for the solid response at the external frequency develops because energy is transferred from the solid to the fluid to drive the fluid oscillations. This energy transfer is not evenly distributed over all frequencies but focuses on the eigenfrequency of the pore fluid oscillations.

Oscillations of the pore fluid decay after their initialization. This decay is different for different reservoir thicknesses and may be used to extract thickness information.

Acknowledgement

We greatly acknowledge the financial support of the Swiss Commission for Technology and Innovation CTI.

References

Bloch, G. and Akrawi, K., 2006, Application of Low Frequency Passive Seismic Surveys in ADCO, UAE: EAGE Workshop Passive Seismic, December 10-13, Dubai, United Arab Emirates

Bourbie, T., Coussy, O. and Zinszner, B., 1987, Acoustics of porous media: Editions Technip, 2-7108-0516-2

Dangel, S., Schaepman, M. E., Stoll, E. P., Carniel, R., Barzandji, O., Rode, E. D. and Singer, J. M., 2003, Phenomenology of tremor-like signals observed over hydrocarbon reservoirs: Journal Of Volcanology And Geothermal Research, 128, 135-158

Graf, R., Schmalholz, S. M., Podladchikov, Y. and Saenger, E., 2007, Passive low frequency spectral analysis: Exploring a new field in geophysics: World Oil, January, 47-52

Hilpert, M., 2007, Capillarity-induced resonance of blobs in porous media: Analytical solutions, Lattice-Boltzmann modeling, and blob mobilization: Journal of Colloid and Interface Science, 309, 493-504

Holzner, R., Eschle, P., Dangel, S., Frehner, M., Narayanan, C. and Lakehal, D., 2007, Hydrocarbon microtremors interpreted as nonlinear oscillations driven by oceanic background waves: Communications in nonlinear science and numerical simulation, topical issue "Geophysics", Submitted

Holzner, R., Eschle, P., Zurcher, H., Lambert, M., Graf, R., Dangel, S. and Meier, P. F., 2005, Applying microtremor analysis to identify hydrocarbon reservoirs: first break, 23, 41-46

Ionescu, D.-C. and Igel, H. [2003] Transparent boundary conditions for wave propagation on unbounded domains. ICCS, Melbourne and St. Petersburg 2003, LNCS 2659, 807-816, Sloot, P.M.A. et al. (Eds), Springer Verlag, Berlin Heidelberg, ISBN: 3-540-40196-2.

Suntsov, A. E., Aroutunov, S. L., Mekhnin, A. M. and Meltchouk, B. Y., 2006, Passive Infra-Frequency Microseismic Technology – Experience and Problems of Practical Use: EAGE Workshop Passive Seismic, December 10-13, Dubai, United Arab Emirates

Virieux, J., 1986, P-Sv-Wave Propagation In Heterogeneous Media - Velocity-Stress Finite-Difference Method: Geophysics, 51, 889-901